Corrosion Assessment of Arc Thermal Sprayed Al and its Alloy Coatings in Aggressive Environments: An Overview

Prakhar Singh

Department of Smart Structure Engineering, Hanyang University, 1271 Sa-3-dong, Sangnok-gu, 15588, Ansan, Republic of Korea. E-mail: prakharvnssingh@gmail.com

Jitendra Kumar Singh

Innovative Durable Building and Infrastructure Research Center,
Center for Creative Convergence Education,
Hanyang University, 1271 Sa-3-dong, Sangnok-gu, 15588, Ansan, Republic of Korea.

Corresponding author: jk200386@hanyang.ac.kr

(Received on June 27, 2024; Revised on July 10, 2024; Accepted on July 10, 2024)

Abstract

Arc thermal sprayed coatings have a wide range of applications, including corrosion resistance, wear resistance, thermal barriers, and electromagnetic pulse protection. However, these coatings often suffer from significant defects and pore formation, which can reduce their overall effectiveness. This overview focuses on the corrosion resistance properties of Al and its alloys. Al coatings demonstrate good corrosion resistance in marine environments due to the formation of sparingly soluble corrosion products on the surface. When Zn is alloyed with Al, the initial corrosion resistance decreases due to an increased number of pores. However, over extended exposure, these coatings exhibit excellent corrosion resistance as corrosion products fill the pores, providing barrier protection. Additionally, incorporating 5 wt.% Mg in Al coatings enhances bond adhesion and improves corrosion resistance in aggressive environments. To further reduce porosity and enhance corrosion resistance, the use of phosphate-based eco-friendly pore sealing agents is discussed. Optimizing the amount of phosphate during treatment is crucial, as it significantly reduces porosity and enhances corrosion resistance. Both insufficient and excessive amounts of phosphate can deteriorate the coating, while the optimal amount improves corrosion resistance over prolonged exposure to aggressive conditions.

Keywords- Corrosion, Coatings, Steel, Pore sealing agent, Arc thermal spray.

1. Introduction

Plain carbon steel, commonly known as mild steel, is a highly versatile material extensively used in construction, offshore structures, ships, pipelines, and bridges. Despite its wide range of applications, it is prone to corrosion, which can compromise its structural integrity over time. To mitigate this issue, various protective schemes are employed, including metallic coatings, heavy-duty paints, polymeric coatings, and high corrosion resistance steel, depending on the exposure conditions such as aqueous, dry, and hot environments. These schemes aim to reduce or slow down the rate of corrosion, ensuring the longevity and safety of steel structures.

Corrosion of steel structures in marine or coastal areas is particularly problematic. In such environments, sacrificial coatings can be more effective than barrier methods like heavy-duty paint or stainless steel. Stainless steel is prone to pitting corrosion, while polymeric coatings can peel off once corrosion starts. Polymeric coatings also have nano-sized pores through which small chloride ions (Cl⁻) can easily penetrate, initiating the corrosion process. Sacrificial coatings are effective for corrosion protection, but the method of deposition is crucial. Common methods for applying these coatings include hot-dip galvanizing (HDG), electroplating, electroless coating, and thermal spray processes.

The arc thermal spray coating process has been in use for decades and is considered more convenient than other coating methods due to the portability of the spray gun, which can be used in various locations for coating application (Jandin et al., 2003). In this process, twin wires serve as consumable materials (feedstock). An electric arc melts these wires, and the molten material is then atomized by hot air, as illustrated in **Figure 1** (Lee et al., 2016). The molten metal particles are subsequently propelled onto the steel substrate by compressed air, where they cool down at room temperature, forming the coating (Pawlowski, 2008). However, due to the rapid cooling and high-speed spraying, the resulting coating often contains pores and defects (Chaliampalias et al., 2008; Choe et al., 2014; Jandin et al., 2003; Paredes et al., 2006). These defects can be mitigated by using a pore sealing agent. Coatings deposited by the arc thermal spray process have a wide range of applications, including corrosion resistance, wear resistance, thermal barriers, and electromagnetic pulse protection (Singh, 2023).

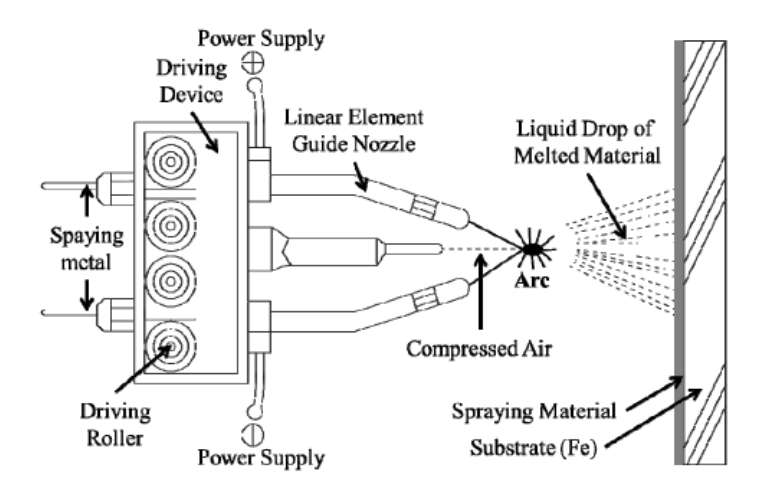


Figure 1. Schematic diagram of the arc thermal metal spay process (Lee et al., 2016).

In this study, we examine the application of various metallic coatings, including aluminum (Al), zinc (Zn), magnesium (Mg), and their alloys, deposited using the arc thermal spray process. We discuss the corrosion resistance properties of these coatings under different corrosive conditions. Additionally, we address the inherent porosity and defects associated with the arc thermal spray process, which can diminish the performance of the coatings. To mitigate these issues, we explore the use of different pore sealing agents.

2. Application of Arc Thermal Sprayed Coating in Marine Conditions

A 300 µm thick coating of different materials—AA1050, AA1100, 85Zn-15Al, and 95Al-5Mg alloys—was deposited on plain carbon steel using the arc thermal spray coating process as shown in **Figure 2** (Grinon-Echaniz et al., 2021). **Figure 2(a)** illustrates the 5% artificial defects in the different metallic coatings, used to determine corrosion resistance in artificial ocean water. **Figure 2(b)** displays the visual appearance of the coatings after 50 days of exposure to artificial ocean water, where the ZnAl coating showed a noticeable color change with white corrosion product deposition. This is attributed to the corrosion of Zn, which is galvanically more active than Al, leading to the formation of Zn oxides/hydroxides/chlorides (Azevedo et al., 2015; Liu et al., 2017). Additionally, these coatings were exposed to different marine environments at the marine Corrosion Test Site "El Bocal" in Santander (Spain) across various zones: atmospheric/splash, tidal, and immersed, for 6 months, as shown in **Figure 2(c)**. The figure reveals that the Al alloy coatings showed no significant change in appearance when exposed to the

atmospheric zone, whereas the ZnAl coating exhibited discoloration due to corrosion product formation. In the tidal zone, the loosely bound corrosion products on the ZnAl coating were washed away. Biofouling was observed on all coatings across the atmospheric to immersed zones, with the ZnAl coating showing the least amount. Rust was detected in the defect areas of the Al alloy coatings in the atmospheric and tidal zones. However, the ZnAl coating did not show any rust in all exposure zones, suggesting that it is more efficient than the Al alloy coatings.

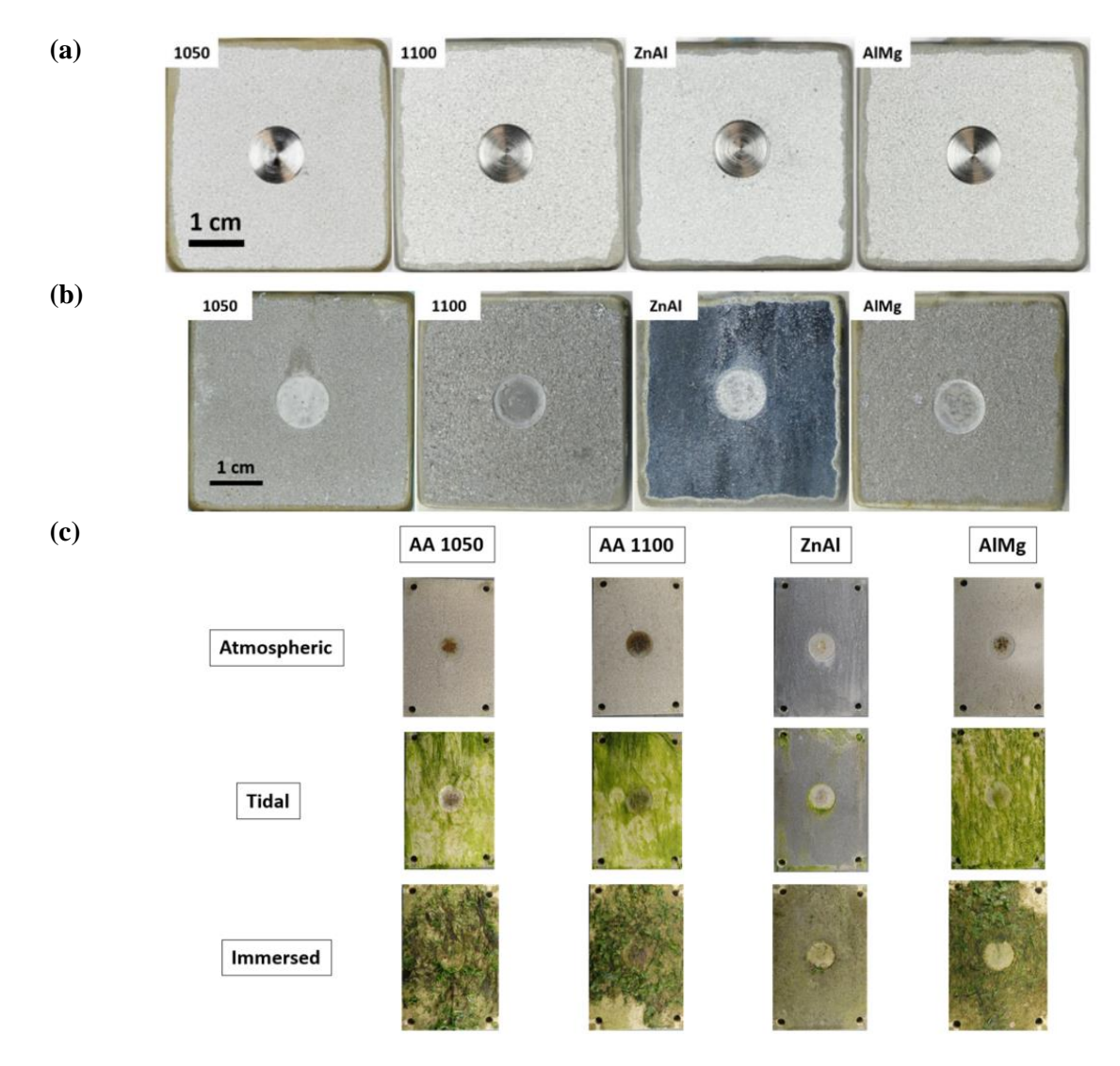


Figure 2. (a) Arc thermal spray coating with 5% surface defects (b) after immersion in artificial ocean water for 50 days, and (c) after 6 months of exposure at E1 Bocal (Spain) in different zones (Grinon-Echaniz et al., 2021).

Huang et al have deposited Zn and ZnAl coatings by arc thermal spray process on vessel Yongle to assess the long term corrosion performance in Southern sea of China (Huang et al., 2023) and they have found that even after 5 years of exposure, there is no red rust on the coating surface as shown in **Figure 3**. The red rust percolate from the steel substrate and come out to the coating surface through the defects/pores of

the coating. Even though there is no bubble, cracks or peel-off phenomena observed. There is white rust deposited onto the coating surface attributed to the formation of oxides/hydroxides of Zn/Al. However, as the exposure duration is extended, the white rust become denser and thicker. The Zn or Al can be used as coating materials to protect the marine structure where sacrificial and barrier protection could be provided (Panossian et al., 2005; Schmidt et al., 2006).

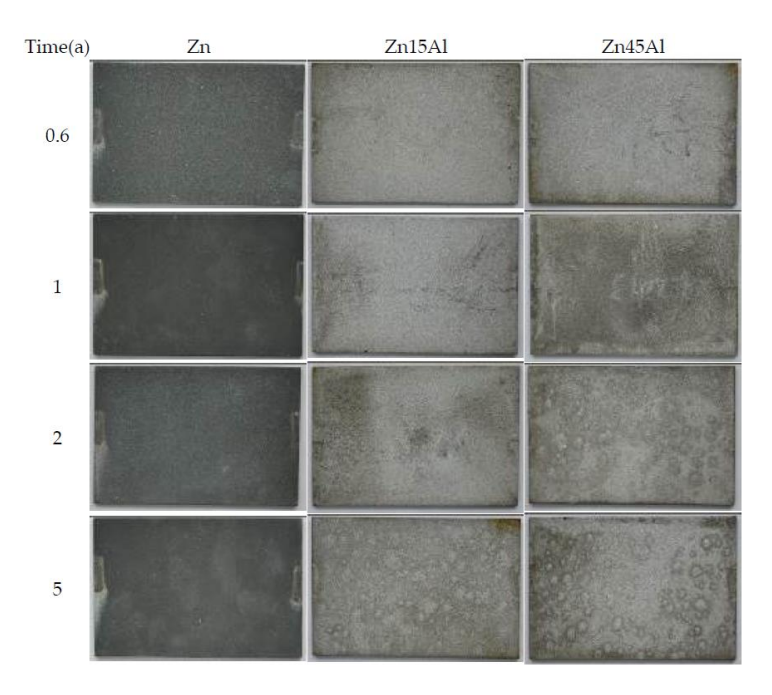


Figure 3. Corrosion morphology changes of the three kinds of coatings deposited by arc thermal spray process and exposed them in Southern Sea of China (Huang et al., 2023).

3. Characterization and Application of Al and Alloys Coating

3.1 Effect of Mg Alloying in Al Coating

The Al coating was deposited by arc thermal spray process and the surface morphology of the coating is shown in **Figure 4(a)**. It can be seen from **Figure 4(a)** that there are many defects and pores observed (Choe et al., 2014; Paredes et al., 2006) as marked by arrow in **Figure 4(a)**. During deposition of the coating, the molten metal particles propelled by high velocity compressed air thereby forming a layer-by-layer plate like morphology (Min-Su et al., 2009) as observed in **Figure 4(a)**. These molten metal particles get cool rapidly at room temperature and form splashed zone (Deshpande et al., 2004; Torres et al., 2007) where moisture and aggressive ions easily penetrate and initiate the corrosion reaction (Celik et al., 2005; Kawakita et al., 2003). The phases formed after deposition of Al coating is shown in **Figure 4(b)**. It can be seen from the XRD results (**Figure 4(b)**) that only Al is observed. It is very interesting to note here that there is no oxide formed, which suggests that the coating deposited by arc thermal spray process reduces the possibility for the oxidation of coatings.

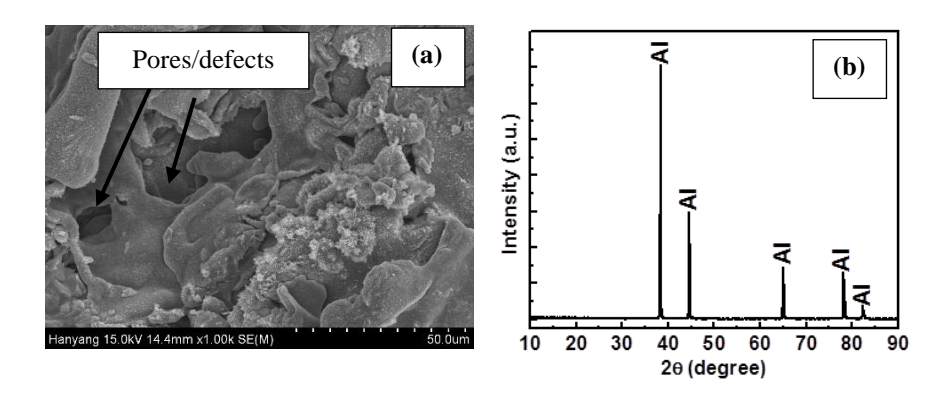


Figure 4. SEM (a) and XRD (b) of the Al coating by the arc thermal metal spray (Lee et al., 2016).

The bond adhesion of pure Al and alloyed with 5Mg i.e. 95Al5Mg alloy coating deposited on steel substrate using thermal spray system was measured by Jeong and Singh (Jeong & Singh, 2023) and the results are shown in **Figure 5**. It can be seen from **Figure 5** that addition of 5% Mg in Al exhibited 38% higher bond adhesion compared to pure Al (Park & Kim, 2016) attributed to the solid solution strengthening during melting (Gupta et al., 2012; Polmear, 2005; Vargel, 2020). This finding suggests that alloying of Mg in Al is better than using pure Al for the deposition of coating and enhance the bond adhesion.

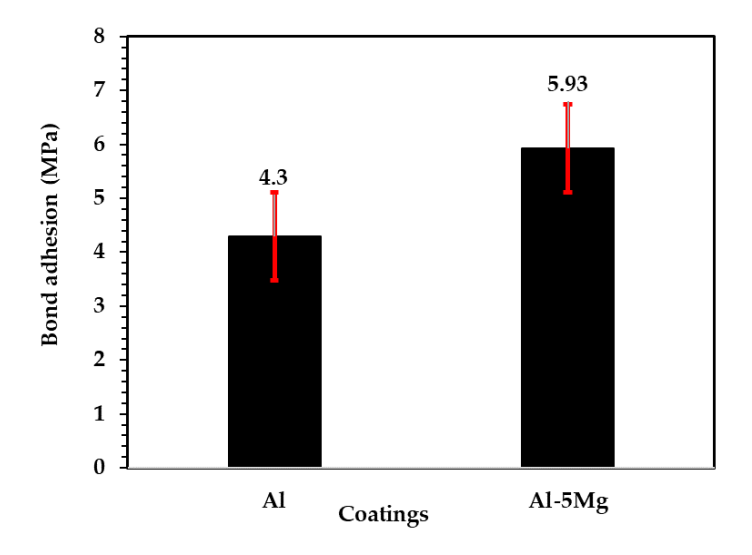


Figure 5. Bond adhesion values of the coatings (Jeong & Singh, 2023).

The corrosion resistance properties of Al and 95Al5%Mg coatings after 41 days of immersion in 3.5 wt.% of NaCl solution was assessed by potentiodynamic polarization and the qualitative and quantitative results are shown in **Figure 6** and **Table 1**, respectively (Jeong & Singh, 2023). It can be seen from **Figure 6** that both coatings exhibit oxygen-reduction reaction during cathodic polarization. However, by considering cathodic current, it can be observed that Al coating shows higher in value compared to alloy might be attributed to the formation of loose oxide film, which reduced during cathodic scanning. The Mg is galvanically more active than Al, which leads to dissolute the coating at greater extend but at the meantime, the corrosion products deposit over the coating surface and fill the defects/pores of the coating (Wang et al., 2022). Therefore, in the quantitative electrochemical analysis (**Table 1**), the corrosion potential (E_{corr}) of 95Al5Mg coating is higher compared to pure Al coating. The corrosion current density (i_{corr}) and

corrosion rate of 95Al5Mg is reduced by around 1.6 times compared to Al coating. This finding suggests that Mg has beneficial effect on corrosion protection for long term application in marine condition.

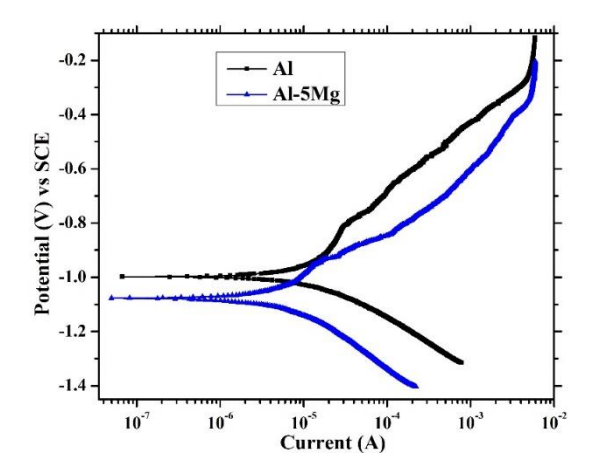


Figure 6. Potentiodynamic polarization plots of coatings after 41 d of immersion in 3.5 wt.% NaCl solution (Jeong & Singh, 2023).

Table 1. Electrochemical parameters of the coating extracted after fitting in Tafel regions (Jeong & Singh, 2023).

Coatings	Electrochemical parameters		
	E _{corr} (V) vs SCE	$i_{corr} (\mu A/cm^2)$	Corrosion rate (µm/year)
Al	-0.99	3.83	41.75
95Al5Mg	-1.09	2.35	26.56

3.2 Effect of Zn with Al on Corrosion Resistance Properties of Coating

As described above that the addition of 5% Mg in Al exhibited excellent corrosion resistance properties. Therefore, it is decided to discuss the role of Zn in Al coating. The surface morphology of the Al-Zn coating exhibited severe defects and pore formation as shown in **Figure 7** (Lee et al., 2019). There are many small inflight particles with splats observed attributed to the sudden cooling and difference in density and melting points of Al and Zn in alloy. There is 3.68% oxygen found in EDS analysis attributed to the atmospheric oxygen, which came after depositing the coating.

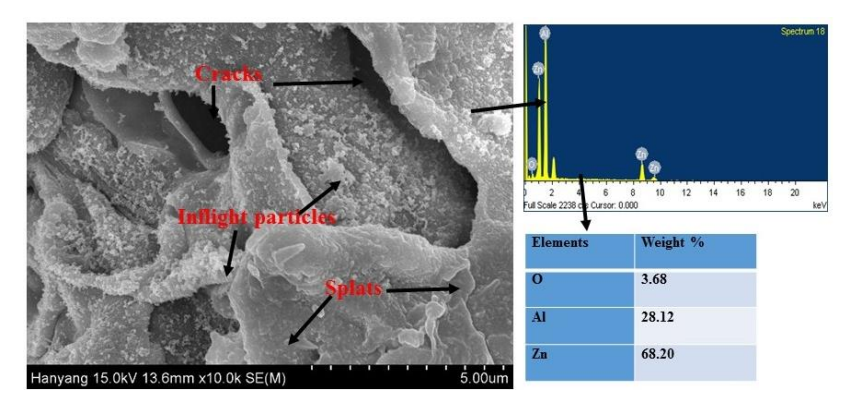


Figure 7. FE-SEM image and EDS of Al-Zn coating (Lee et al., 2019).

The XRD analysis of Al-Zn alloy coating is shown in **Figure 8** (Lee et al., 2019). It can be seen from this **Figure 8** that Al (JCPDS: 85–1327) and Zn (JCPDS: 87–0713) is observed. This result suggests that there is no oxidation of the coating during deposition by arc thermal spray process.

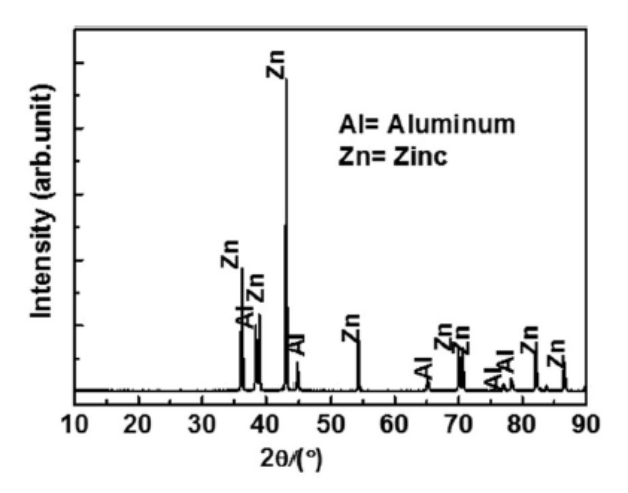


Figure 8. XRD of Al-Zn coating (Lee et al., 2019).

The polarization resistance (R_p) and capacitance (C_{eff}) of the coating over various exposure periods in a 3.5 wt.% NaCl solution are shown in **Figure 9** (Lee et al., 2019). The figure reveals that the R_p value gradually increases up to 13 days. Beyond this period, there is a dramatic increase in R_p , which then stabilizes after 40 days of exposure. This behavior is attributed to the deposition of corrosion products in the coating's defects and pores, providing a barrier type of protection. Initially, the active centers of the coating (pores/defects) promote dissolution reactions, resulting in the lowest R_p values. As these active centers are consumed during exposure, corrosion products form and deposit over the surface, increasing corrosion resistance. Consequently, the C_{eff} value is initially very high due to defects in the coating. However, as corrosion products reduce the active centers, the C_{eff} value decreases dramatically and stabilizes after 40 days of exposure.

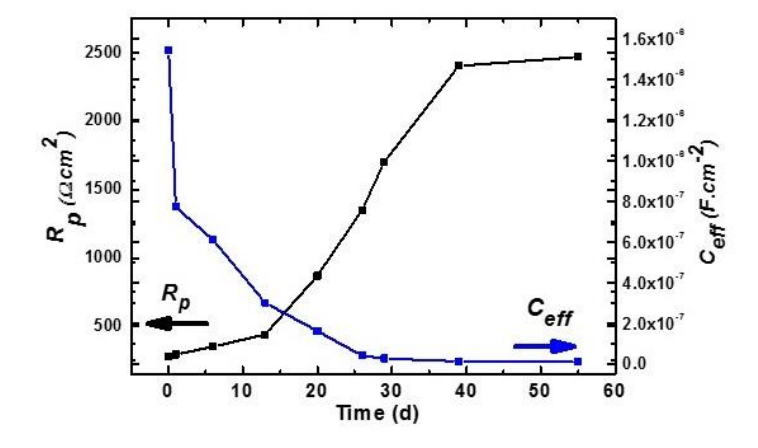


Figure 9. Plot between Rp and Ceff against time exposed to 3.5 wt.% NaCl solution (Lee et al., 2019).

The corrosion protection offered by Al-Zn coating during extended exposure in a 3.5 wt.% NaCl solution is illustrated schematically in **Figure 10** (Lee et al., 2019). The figure outlines the different stages from

coating deposition to prolonged exposure. Initially, the coating is deposited using an arc thermal spray process, resulting in the formation of significant defects and pores. These active centers facilitate the initiation of the corrosion reaction. When the solution comes into contact with the coating, these defects and pores enable the onset of corrosion and the formation of corrosion products (step 2). In the initial stages of exposure, the coating dissolves, and corrosion products begin to form and deposit over the surface. Over an extended duration of exposure, these corrosion products create a barrier that prevents the penetration of aggressive ions, thereby reducing the corrosion rate (step 3).

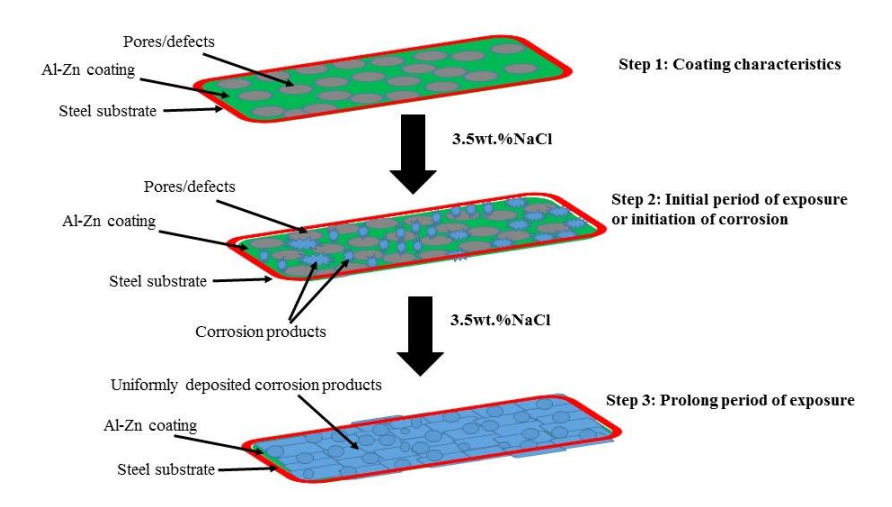


Figure 10. Schematic presentation of corrosion process of Al-Zn coating applied by arc thermal spray process in 3.5 wt.% NaCl solution with exposure periods (Lee et al., 2019).

4. Application of Pore Sealing Agent to Fill the Defects of the Coating

As we have observed above that Al coating deposited by arc thermal spray process exhibited defects and pores formation and reduce the performance of the coating. Therefore, it is utmost required to fill the defects and pores of the deposited coating using eco-friendly and economical pore sealing agents. Lee et al have used ammonium phosphate (AP) as pore sealing agent for Al to reduce the porosity and enhance the corrosion resistance performance at longer duration of exposure (Lee et al., 2017). They have selected different concentration of ammonium phosphate i.e. 0.1 M (AP1), 0.5 M (AP2) and 1 M (AP3) solution and applied by brush three times in a day and subsequently kept them in humidity chamber at 50 °C and 95% relative humidity for 7 days to create the natural atmosphere for the corrosion performance evaluation. The surface morphology of the treated and as coated (AC) samples is shown in **Figure 11**. The Al coating treated with AP1 solution exhibited elongated needle like morphology (Figure 11(a)), which uniformly cover the surface of Al by forming a composite oxide. Moreover, as the amount of AP is increased, the morphology of the oxide film is differed. In the case of AP2, the length of needle like particle is decreased as well as some plate like morphology is seen in **Figure 11(b)**. There is dramatic change in the morphology of the composite oxide of AP3 solution treated sample where micro crack and chunk like morphology is observed attributed to the brittle nature of the film, which leads to cause the corrosion (Lee et al., 2016a; Lee et al., 2016b). The phosphate ions (from AP) has greater affinity to react with Al and form aluminum phosphate but high amount of phosphate ions leads to form a brittle film of metal phosphate (Imaz et al., 2014; Tang & Zuo, 2008), therefore, crack is observed in AP3 (Figure 11(c)).

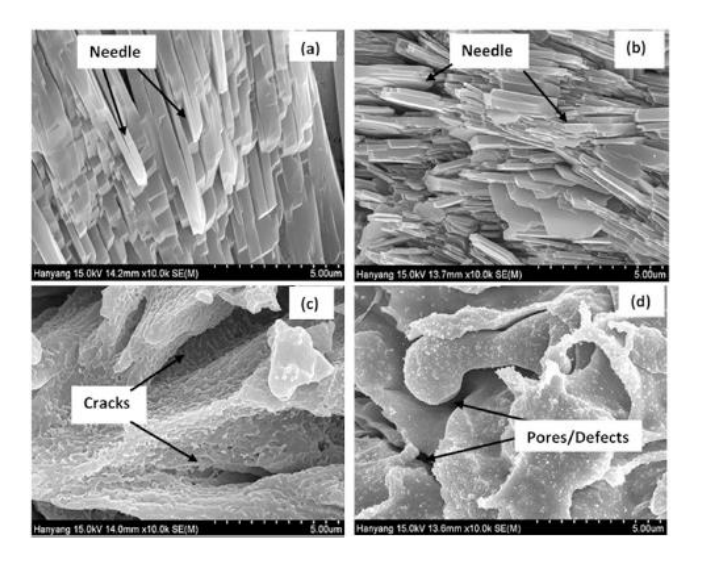


Figure 11. SEM images of Al coating applied by arc thermal spray process (a) AP1, (b) AP2, (c) AP3 and (d) AC (Lee et al., 2017).

The corrosion resistance properties of post-treated Al coatings with varying amounts of AP solution after 60 days of continuous immersion in artificial ocean water are shown in **Figure 12**, with the electrochemical data after fitting in the Tafel region provided in **Table 2** (Lee et al., 2017). The corrosion current density and potential for the AP1 samples are the lowest and shifted towards the nobler direction, respectively, due to the formation of a passive oxide film (Yao et al., 2013). The cathodic and anodic currents of the AP1 coating are lower than those of other samples after 60 days of immersion, indicating that a lower amount of AP solution provides superior corrosion resistance compared to higher amounts. Conversely, the anodic current density of the AP3 sample dramatically increases after E_{corr}, suggesting the presence of pits in the coating due to a brittle film that dissolves over 60 days of exposure. The quantitative electrochemical data reveal that the AP3 sample exhibits an active E_{corr} and the highest i_{corr}, indicating a higher susceptibility to corrosion and dissolution. The i_{corr} of the AP1 sample is reduced by more than nine times compared to the AC sample, demonstrating that a 0.1 M AP solution is highly effective in controlling the corrosion of Al coatings and enhancing corrosion resistance over extended exposure in a marine environment.

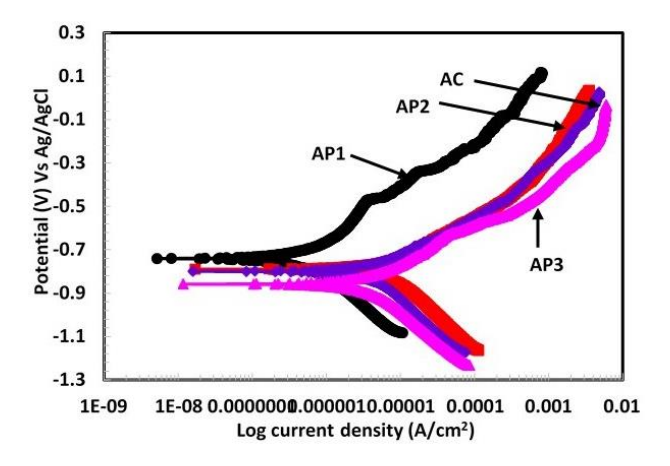


Figure 12. Potentiodynamic plots of treated and AC Al coating applied by arc thermal spray process in artificial ocean water after 60 days of exposure (Lee et al., 2017).

AP1 AP2

AP3

7.83

8.65

Tafel regions after 60 days of exposure in artificial ocean water (Lee et al., 2017).				
Coatings	Electrochemical parameters			
	E _{corr} (V) vs Ag/AgCl	$i_{corr} (\mu A/cm^2)$		

-0.793

-0.781

-0.850

Table 2. Electrochemical parameters of Al coating were extracted after fitting of potentiodynamic plots	1n
Tafel regions after 60 days of exposure in artificial ocean water (Lee et al., 2017).	

The AP acts as an agent to address pores and defects in Al coatings, significantly reducing porosity and enhancing corrosion resistance. This process is detailed by Lee et al. in the schematic shown in Figure 13 (Lee et al., 2017). Initially, pores and defects form after depositing the Al coating on the steel substrate. The AP solution is then used to fill these defects and reduce porosity. The surface treatment with AP solution is performed three times within 24 hours, followed by placing the treated samples in a humidity chamber at 50°C and 95% relative humidity for 7 days to allow natural oxides to form, as typically observed in open air. After removal from the humidity chamber, a composite oxide, aluminum hydrogen phosphate (AHP), forms over the coating surface, reducing porosity (step 2). When the post-treated coating is immersed in artificial ocean water for corrosion resistance testing, the AHP transforms into aluminum hydroxide phosphate hydrate (AHPH) over extended exposure (step 3). AHPH is highly stable and exhibits excellent corrosion resistance.

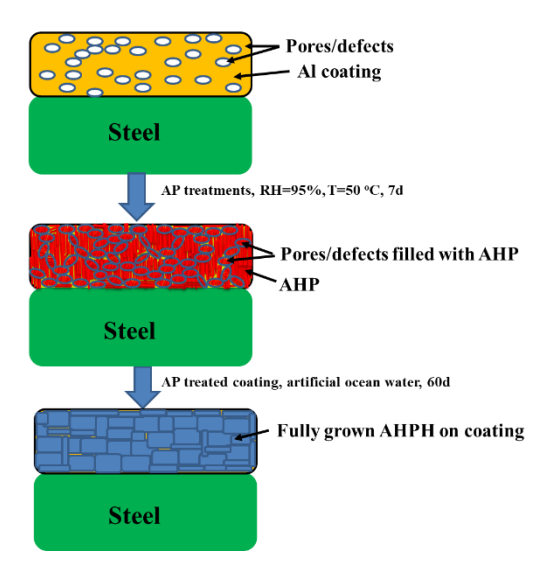


Figure 13. Illustration of schematic diagram for corrosion process of AP treated Al coating exposing them in artificial ocean water after 60 days (Lee et al., 2017).

As above described that AP has exhibited excellent corrosion resistance properties in 0.1 M concentration. Therefore, it was decided by Lee et.al to select the other eco-friendly pore sealing agent to improve the properties of Al coating deposited by arc thermal spray process (Lee et al., 2020). Different amount of NaH₂PO₄ along with a fixed amount of Ca(NO₃)₂ has been used to reduce the porosity of as coated (AC) samples and studied the corrosion resistance properties at longer duration of exposure in 3.5 wt.% NaCl solution. The surface morphology of AC and post-treated Al coating is shown in Figure 14 (Lee et al., 2020). The AC sample exhibited lamellar and cracks in the coating (**Figure 14(a**)) due to the sudden cooling of the molten metal particle during deposition. The particle size of the lamellae is found around 5-10 µm.

However, once the Al coating is treated with pore sealing agent, the morphology of the coating is changed attributed to the formation of composite oxides on the surface. The coating treated with SPCN1 solution, it shows non-homogeneous filamentous and cluster of needle (Jeong et al., 2019; Lee & Singh, 2019) as shown in **Figure 14(b)** attributed to the lower amount of NaH₂PO₄. However, once the amount of NaH₂PO₄ with 0.1 M Ca(NO₃)₂ is increased, the coating become dense and size of the needle like oxides is decreased attributed to the greater amount of phosphate where Ca act as precursor for making dense and compact morphology (Natarajan & Rajeswari, 2008). At the high concentration of NaH₂PO₄ solution, there is microcrack observed in the coating (**Figure 14(d)**) attributed to the greater amount of phosphate, which leads to create the crack (Jeong et al., 2019). The porosity of the coating is calculated and it is found to be 31, 25, 19 and 9% for AC, SPCN1, SPCN2, and SPCN3, which is reduced by 19, 38 and 71% compared to AC, respectively.

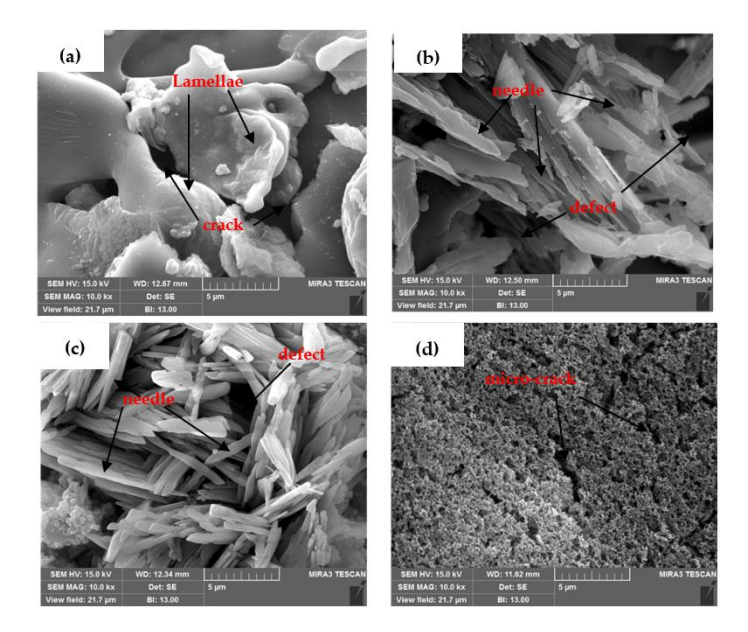


Figure 14. SEM of (a) as coated (AC), (b) $0.1 \text{ M NaH}_2\text{PO}_4 + 0.1 \text{ M Ca(NO}_3)_2 (SPCN1)$, (c) $0.5 \text{ M NaH}_2\text{PO}_4 + 0.1 \text{ M Ca(NO}_3)_2 (SPCN2)$, and (d) $1 \text{ M NaH}_2\text{PO}_4 + 0.1 \text{ M Ca(NO}_3)_2 (SPCN3)$ (Lee et al., 2020).

The corrosion studies of these coating is assessed in 3.5 wt.% NaCl solution at extended duration of exposure and the resistance to coating/treatment (R_{c/l}) and C_{eff} results are shown in **Figure 15** (Lee et al., 2020). It can be seen from **Figure 15** that of all sample's R_{c/l} is gradually increased except SPCN3. Once the SPCN3 sample kept in solution, the composite oxides formed after treatment i.e. brushite (BR) and sodium aluminum hydrogen phosphate (SAHP) dissolute and make the studied solution acidic, therefore, this value is decreased. It is interesting to note here that the AC sample exhibit higher in R_c value after 41 days of exposure compared to SPCN1 and SPCN3 attributed to the greater pore filling ability by the corrosion product formed until these periods while in the case of SPCN1, the BR and SAHP is not in optimum amount and dissolved. In the case of SPCN3, the BR and SAHP are formed significantly but make the studied solution acidic and enhances the dissolution reaction. However, in the case of SPCN2, the BR and SAHP formed in optimum amount and transformed into stable corrosion products during immersion periods, therefore, it exhibits highest in amount. The C_{eff} is inversely proportion to R_{c/t}, therefore, once R_{c/t} is greater then, C_{eff} is lower. The above finding suggests that to get highest corrosion resistance, it is very important to optimize the amount of pore sealing agents i.e. phosphate based.

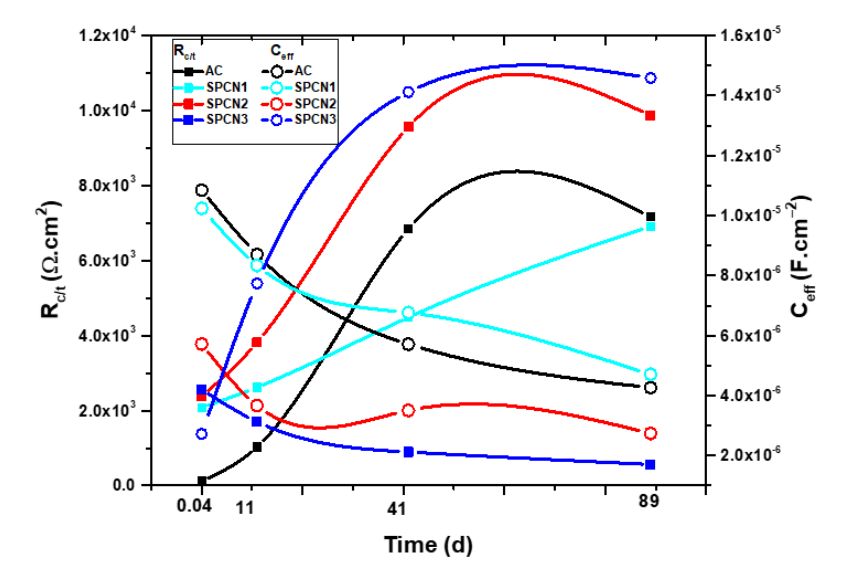


Figure 15. Electrochemical parameters plot of *Rc/t* and *Ceff* with exposure periods in 3.5 wt.% NaCl solution (Lee et al., 2020).

5. Conclusion

This overview discusses the deposition of various metallic coatings using the arc thermal spray process, their characterization, and corrosion resistance properties in different aggressive environments. Arc thermal sprayed coatings develop defects and pores due to the rapid cooling of molten metal particles, which are randomly deposited on the steel substrate. Alloy coatings tend to have more pores due to differences in the melting points and densities of the metals. Zn and its alloys provide cathodic protection in marine conditions due to the galvanic activity of Zn. In contrast, Al and its alloys show enhanced corrosion resistance due to the formation of sparingly soluble and adherent corrosion products. The incorporation of Mg and Zn in Al coatings results in greater corrosion resistance than pure Al coatings, attributed to galvanic coupling that causes the dissolution of the active metal, which then deposits in the pores and creates a barrier. Phosphate-based pore sealing agents significantly reduce the porosity of Al coatings and improve corrosion resistance. However, it is crucial to optimize the amount of phosphate-based sealing agent for the best corrosion resistance. Both insufficient and excessive amounts can deteriorate the coating. Therefore, selecting the appropriate alloy coating for a specific application and the optimal amount of eco-friendly pore sealing agent is essential for achieving excellent corrosion resistance.

Conflict of Interests

The author declares there is no conflict of interest.

Acknowledgments

Not available.

References

Azevedo, M.S., Allély, C., Ogle, K., & Volovitch, P. (2015). Corrosion mechanisms of Zn (Mg, Al) coated steel: 2. The effect of Mg and Al alloying on the formation and properties of corrosion products in different electrolytes. *Corrosion Science*, 90, 482-490.



- Celik, E., Ozdemir, I., Avci, E., & Tsunekawa, Y. (2005). Corrosion behaviour of plasma sprayed coatings. *Surface and Coatings Technology*, 193(1-3), 297-302.
- Chaliampalias, D., Vourlias, G., Pavlidou, E., Stergioudis, G., Skolianos, S., & Chrissafis, K. (2008). High temperature oxidation and corrosion in marine environments of thermal spray deposited coatings. *Applied Surface Science*, 255(5), 3104-3111.
- Choe, H.B., Lee, H.S., & Shin, J.H. (2014). Experimental study on the electrochemical anti-corrosion properties of steel structures applying the arc thermal metal spraying method. *Materials*, 7(12), 7722-7736.
- Deshpande, S., Kulkarni, A., Sampath, S., & Herman, H. (2004). Application of image analysis for characterization of porosity in thermal spray coatings and correlation with small angle neutron scattering. *Surface and Coatings Technology*, 187(1), 6-16.
- Grinon-Echaniz, R., Paul, S., Thornton, R., Refait, P., Jeannin, M., & Rodriguez, A. (2021). Prediction of thermal spray coatings performance in marine environments by combination of laboratory and field tests. *Coatings*, 11(3), 320. https://doi.org/10.3390/coatings11030320.
- Gupta, R., Sukiman, N., Cavanaugh, M., Hinton, B., Hutchinson, C., & Birbilis, N. (2012). Metastable pitting characteristics of aluminium alloys measured using current transients during potentiostatic polarisation. *Electrochimica Acta*, 66, 245-254.
- Huang, G.S., Li, Z.L., Zhao, X.S., Xin, Y.L., Ma, L., Sun, M.X., & Li, X.B. (2023). Degradation behavior of arcsprayed zinc aluminum alloy coatings for the vessel yongle in the south China sea. *Coatings*, *13*(7), 1139.
- Imaz, N., Ostra, M., Vidal, M., Díez, J., Sarret, M., & Lecina, E.G. (2014). Corrosion behaviour of chromium coatings obtained by direct and reverse pulse plating electrodeposition in NaCl aqueous solution. *Corrosion Science*, 78, 251-259.
- Jandin, G., Liao, H., Feng, Z., & Coddet, C. (2003). Correlations between operating conditions, microstructure and mechanical properties of twin wire arc sprayed steel coatings. *Materials Science and Engineering: A*, 349(1-2), 298-305.
- Jeong, H.R., Lee, H.S., Jalalzai, P., Kwon, S.J., Singh, J.K., Hussain, R. R., Aslam, F. (2019). Sodium phosphate post-treatment on Al coating: Morphological and corrosion study. *Journal of Thermal Spray Technology*, 28(7), 1511-1531.
- Jeong, H.R., & Singh, J.K. (2023). Role of 5 wt.% Mg alloying in Al on corrosion characteristics of Al-Mg coating deposited by plasma arc thermal spray process. *Materials*, 16(8), 3088.
- Kawakita, J., Kuroda, S., Fukushima, T., & Kodama, T. (2003). Corrosion resistance of HVOF sprayed HastelloyC nickel base alloy in seawater. *Corrosion Science*, *45*(12), 2819-2835.
- Lee, H.S., Kumar, A., Mandal, S., Singh, J.K., Aslam, F., Alyousef, R., & Albduljabbar, H. (2020). Effect of sodium phosphate and calcium nitrate sealing treatment on microstructure and corrosion resistance of wire arc sprayed aluminum coatings. *Coatings*, 10(1), 33.
- Lee, H.S., & Singh, J.K. (2019). Influence of calcium nitrate on morphology and corrosion characteristics of ammonium phosphate treated Aluminum coating deposited by arc thermal spraying process. *Corrosion Science*, 146, 254-268.
- Lee, H.S., Singh, J.K., & Ismail, M.A. (2017). An effective and novel pore sealing agent to enhance the corrosion resistance performance of Al coating in artificial ocean water. *Scientific Reports*, 7(1), 1-22.
- Lee, H.S., Singh, J.K., Ismail, M.A., & Bhattacharya, C. (2016a). Corrosion resistance properties of aluminum coating applied by arc thermal metal spray in SAE J2334 solution with exposure periods. *Metals*, 6(3), 55. https://doi.org/10.3390/met6030055.



- Lee, H.S., Singh, J.K., Ismail, M.A., Bhattacharya, C., Seikh, A.H., Alharthi, N., & Hussain, R.R. (2019). Corrosion mechanism and kinetics of Al-Zn coating deposited by arc thermal spraying process in saline solution at prolong exposure periods. *Scientific Reports*, 9(1), 1-17.
- Lee, H.S., Singh, J.K., & Park, J.H. (2016b). Pore blocking characteristics of corrosion products formed on Aluminum coating produced by arc thermal metal spray process in 3.5 wt.% NaCl solution. *Construction and Building Materials*, 113, 905-916.
- Liu, S., Zhao, X., Zhao, H., Sun, H., & Chen, J. (2017). Corrosion performance of zinc coated steel in seawater environment. *Chinese Journal of Oceanology and Limnology*, 35(2), 423-430.
- Min-Su, H., Yong-Bin, W., Cheol, K.S., Jeong, Y.J., Ki, J.S., & Jong, K.S. (2009). Effects of thickness of Al thermal spray coating for STS 304. *Transactions of Nonferrous Metals Society of China*, 19(4), 925-929.
- Natarajan, U.V., & Rajeswari, S. (2008). Influence of calcium precursors on the morphology and crystallinity of solgel-derived hydroxyapatite nanoparticles. *Journal of Crystal Growth*, 310(21), 4601-4611.
- Panossian, Z., Mariaca, L., Morcillo, M., Flores, S., Rocha, J., Peña, J., Herrera, F., Corvo, F., Sanchez, M., Rincon, O.T., Pridybailo, G., Rincon, O. (2005). Steel cathodic protection afforded by zinc, aluminium and zinc/aluminium alloy coatings in the atmosphere. *Surface and Coatings Technology*, 190(2-3), 244-248.
- Paredes, R.S., Amico, S., & d'Oliveira, A. (2006). The effect of roughness and pre-heating of the substrate on the morphology of aluminium coatings deposited by thermal spraying. *Surface and Coatings Technology*, 200(9), 3049-3055.
- Park, I.C., & Kim, S.J. (2016). Electrochemical characteristics in seawater for cold thermal spray-coated Al–Mg alloy layer. *Acta Metallurgica Sinica (English Letters)*, 29, 727-734.
- Pawlowski, L. (2008). The science and engineering of thermal spray coatings. John Wiley & Sons, USA.
- Polmear, I. (2005). Light alloys: From traditional alloys to nanocrystals. Elsevier, UK.
- Schmidt, D., Shaw, B., Sikora, E., Shaw, W., & Laliberte, L. (2006). Corrosion protection assessment of sacrificial coating systems as a function of exposure time in a marine environment. *Progress in Organic Coatings*, 57(4), 352-364.
- Singh, J.K. (2023). Application of arc thermal spray process in corrosion protection of steels and electromagnetic pulse shielding. *Prabha Materials Science Letter* 2(2), 75-89
- Tang, J., & Zuo, Y. (2008). Study on corrosion resistance of palladium films on 316L stainless steel by electroplating and electroless plating. *Corrosion Science*, 50(10), 2873-2878.
- Torres, B., Campo, M., Ureña, A., & Rams, J. (2007). Thermal spray coatings of highly reinforced aluminium matrix composites with sol–gel silica coated SiC particles. *Surface and Coatings Technology*, 201(16-17), 7552-7559.
- Vargel, C. (2020). Corrosion of aluminium: Elsevier.
- Wang, Y., Liu, H., Jia, Z., Yang, B., & He, L. (2022). The electrochemical performance of Al-Mg-Ga-Sn-xBi alloy used as the anodic material for Al-air battery in KOH electrolytes. *Crystals*, *12*(12), 1785.
- Yao, Y., Zhao, C., Han, Y., & Zhao, C. (2013). Preparation and corrosion resistance property of Molybdate conversion coatings containing SiO2 nanoparticles. *Journal of The Electrochemical Society*, 160(6), C185.



The original content of this work is copyright © Ram Arti Publishers. Uses under the Creative Commons Attribution 4.0 International (CC BY 4.0) license at https://creativecommons.org/licenses/by/4.0/

Publisher's Note- Ram Arti Publishers remains neutral regarding jurisdictional claims in published maps and institutional affiliations.